High-throughput drug profiling with voltage- and calcium-sensitive fluorescent probes in human iPSC-derived cardiomyocytes

Stephane Bedut,[1,2] Christine Seminatore-Nole,[1] Veronique Lamamy,[2] Sarah Caignard,[2] Jean A. Boutin,[2] Olivier Nosjean,[2] Jean-Philippe Stephan,[2] and Francis Coge[2]

[1]*Laboratoire SERVIER de Chemogénétique, Institut du Cerveau et de la Moelle, Hôpital de la Salpétrière, Paris, France;*
[2]*Pôle d'Expertise Biotechnologie, Chimie & Biologie, Institut de Recherches SERVIER, Croissy-sur-Seine, France*

Bedut S, Seminatore-Nole C, Lamamy V, Caignard S, Boutin JA, Nosjean O, Stephan JP, Coge F. High-throughput drug profiling with voltage- and calcium-sensitive fluorescent probes in human iPSC-derived cardiomyocytes. *Am J Physiol Heart Circ Physiol* 311: H44–H53, 2016. First published May 3, 2016; doi:10.1152/ajpheart.00793.2015.—Cardiomyocytes derived from human embryonic stem cells (hESCs) or induced pluripotent stem cells (hiPSCs) are increasingly used for in vitro assays and represent an interesting opportunity to increase the data throughput for drug development. In this work, we describe a 96-well recording of synchronous electrical activities from spontaneously beating hiPSC-derived cardiomyocyte monolayers. The signal was obtained with a fast-imaging plate reader using a submillisecond-responding membrane potential recording assay, FluoVolt, based on a newly derived voltage-sensitive fluorescent dye. In our conditions, the toxicity of the dye was moderate and compatible with episodic recordings for >3 h. We show that the waveforms recorded from a whole well or from a single cell-sized zone are equivalent and make available critical functional parameters that are usually accessible only with gold standard techniques like intracellular microelectrode recording. This approach allows accurate identification of the electrophysiological effects of reference drugs on the different phases of the cardiac action potential as follows: fast depolarization (lidocaine), early repolarization (nifedipine, Bay K8644, and veratridine), late repolarization (dofetilide), and diastolic slow depolarization (ivabradine). Furthermore, the data generated with the FluoVolt dye can be pertinently complemented with a calcium-sensitive dye for deeper characterization of the pharmacological responses. In a semiautomated plate reader, the two probes used simultaneously in 96-well plates provide an easy and powerful multiparametric assay to rapidly and precisely evaluate the cardiotropic profile of compounds for drug discovery or cardiac safety.

96-well plate; cell signaling; cardiomyocytes; induced pluripotent stem cells; membrane potentials

NEW & NOTEWORTHY

We describe 96-well recording of synchronous electrical activities from spontaneously beating human induced pluripotent stem cell-derived cardiomyocyte monolayers using FluoVolt as a substitute for patch-clamp measurements, validated with reference pharmacological compounds to demonstrate the usefulness of the approach.

HEART DISEASES REMAIN a major public health concern, and cardiac adverse events are the main reason for compound attrition during drug development or withdrawals after approval. Therefore, the need for predictive high-throughput drug screening and profiling is increasingly critical for efficient drug discovery and development. In this context, human embryonic stem cell (hESC)-derived and induced pluripotent stem cell (hiPSC)-derived cardiomyocytes are of growing interest. Recent progress in stem cell biology has revealed human cell-derived models as promising tools for drug discovery and development, especially for toxicity studies (26). When adequately differentiated, hESC- and hiPSC-derived cells give rise to spontaneously beating cells with cardiomyocyte-like electrophysiological activities (6, 14) as well as calcium homeostasis (27), offering an attractive opportunity for in vitro assays (26). Although the phenotype of these cardiomyocytes is described as immature, they provide relevant information for drug profiling (1, 3).

Gold standard study methods like patch-clamp recording from isolated cardiomyocytes or heterologous expression systems are required to evaluate the cardiac electrophysiological impact of compounds. However, these techniques are time-consuming and not adapted to high-throughput data generation for systematic tests or screening libraries of compounds. Efforts have been carried out to develop high-throughput assays based on field potential (1, 7) and/or impedance recording (5, 9, 10) to investigate hESC/hiPSC-derived cardiomyocyte monolayer electrical and mechanical activities, respectively, and have proved to be good approaches for identifying drug-induced cardiotropic effects of compounds (8). However, these kinds of assays can be technically challenging and fairly difficult to implement considering the required investment in dedicated devices.

Other recording techniques rely on fluorescent dyes for the optical measurement of calcium and electrical cardiomyocyte activities. A fluorescent calcium-sensitive dye combined with a high-content imaging system and a high-throughput automated optical device was previously shown to provide useful results for drug characterization (18). More direct electrophysiological recordings have also been performed on hiPSC-derived cardiomyocytes using voltage-sensitive genetically encoded (12) or organic (13) dyes. In addition, a microscope-based imaging station able to simultaneously record both electrical and calcium activities from a hiPSC-derived cardiomyocyte monolayer through the use of fluorescent dyes has been described (11). However, optical action potential recording can present some issues related to the nature and properties of the voltage-sensitive dye used for the assay. Genetically encoded dyes like ArcLight, in addition to the need for a transfection phase, suffer from a lagging response to fast membrane potential variation that can alter the time course of the signal (12). Organic electrochromic dyes like those of the ANEPPS family are fast responding but show a rapid cellular phototoxicity that

develops proportionally to the intensity and duration of the illumination and thus limits their use (25).

Recently, a new family of fast voltage-responding fluorescent molecules was described (15). These molecules take advantage of photoinduced electron transfer modulation, allowing submillisecond responses to membrane voltage changes and higher signal dynamics than commonly used electrochromic dyes (15). In this work, we aimed to develop a simple and high-throughput method to record the spontaneous electrical activity of a hiPSC-derived cardiomyocyte monolayer in 96-well format using a new fast voltage-responding fluorescent molecule based on this principle. We evaluated the FluoVolt (FV) probe in terms of toxicity, sensibility to cell density, DMSO susceptibility, and accuracy for cardiotropic drug effect detection. Ultimately, we demonstrate the advantage of combining FV and calcium activity recording for the semiautomated evaluation of the cardiac electrophysiological profile of compounds on hiPSC-derived cardiomyocytes.

MATERIALS AND METHODS

Human iPSC-derived cardiomyocyte culture and plating. Two hiPSC-derived cardiomyocyte cell lines were used for this study. Human iPSC-derived iCell cardiomyocytes were purchased from Cellular Dynamics International (CDI, Madison, WI) and processed according to the manufacturer's protocol. Briefly, cells were thawed in CDI plating media and seeded onto Millicell eight-well glass slides coated with fibronectin (Millipore, Billerica, MA) for microscopy studies. Each vial was thawed in a 37°C water bath, and cardiomyocytes were transferred into a 50-ml tube and diluted with plating medium (iCell Cardiomyocyte Plating Medium) at a concentration of $20-25 \times 10^3$ cells/well per 100 μl. Cells were placed in a 96-well plate (655090 Cellstar; Greiner Bio-One, Kremsmünster, Austria) precoated with 10 μg/cm^2 fibronectin (F0895; Sigma-Aldrich, St. Louis, MO) at a concentration of $20-25 \times 10^3$ cells/well per 100 μl. Cells were maintained in a 5% CO_2 incubator at 37°C, and culture media were replaced every 2–3 days. Cardiomyocytes were used 10–12 days after plating. The cardiomyocyte cell line Cor.4U (Axiogenesis, Köln, Germany) was kindly provided by Axiogenesis as a fully seeded and ready-to-use 96-well plate with a cell density at 3×10^4 cells per well. The Axiogenesis culture medium was changed upon cell arrival, and the cells were used on the following days.

Drugs and solutions. All experiments were carried out in an experimental solution composed of Hank's balanced salt solution (Life Technologies, Carlsbad, CA) supplemented with 20 mM HEPES (Life Technologies), and pH was adjusted to 7.4 with NaOH. DMSO, nifedipine, dofetilide, Bay K8644, lidocaine, and ouabain were purchased from Sigma-Aldrich, veratridine was purchased from Tocris (Bristol, United Kingdom), and ivabradine was provided by the Servier Research Institute (Suresnes, France) as a chlorhydrate salt. All drugs were solubilized in DMSO as a stock solution and diluted to the final desired concentration in the experimental solution without exceeding 0.3% DMSO.

Microscope-based FV signal imaging. The hiPSC-derived cardiomyocytes were seeded in a Millicell eight-well glass slide that was maintained with vacuum grease at the bottom of a Petri dish filled with experimental solution at 37°C. The temperature during the experiment was not regulated, so recordings were promptly performed in a large volume of warmed medium to ensure above room temperature conditions. The Petri dish was placed on the stage of an Examiner Z1 upright microscope (Zeiss, Oberkochen, Germany), and observations were made with a ×20 immersed objective in fluorescence at 500–550 nm evoked by excitation at 450–490 nm with an X-Cite 120 PC light source (Exfo, Quebec, Canada). The FV signal was recorded with an EMCCD Evolve 512 camera (Photometrics, Tucson, AZ) controlled with SlideBook 5.0 software (3i, Göttingen, Germany) at a sampling interval between 30 and 50 ms. Analysis was performed with ImageJ 1.47 freeware (National Institutes of Health, Bethesda, MD).

Similarly, the influence of the FV dye concentration on the quality of the signal was tested with six decreasing concentrations that corresponded to the undiluted initial concentration (d1) and its two-, three-, four-, five-, and sixfold dilutions (d2, d3, d4, d5, and d6, respectively). The dose-dependent toxicity of the dye was also evaluated over time through seven recordings of 40 s in length every 30 min in triplicate.

Membrane potential and calcium transient fluorescence signal recording. Electrical activity was recorded using the FV voltage-sensitive dye kit (Molecular Probes, Eugene, OR). A single vial containing the dye was diluted in 100 μl of PowerLoad (a solubilizing agent provided in the FV kit) and then resuspended in 10 ml of experimental medium warmed at 37°C according to the manufacturer's recommendation (there is no indication of the resulting concentration). The dye was also used at higher dilutions as described in RESULTS. The background suppressor furnished in the kit was not added because our conditions did not require it. Calcium activity was recorded with the intracellular calcium-sensitive dye fluo-4 AM (Molecular Probes, Eugene, OR) or CAL520 (AAT Bioquest, Sunnyvale, CA). A total of 50 μg of the dye was diluted in 10 μl DMSO and then diluted in 15 ml of experimental medium warmed at 37°C for a final concentration of ~3 μM. After removal of the culture medium and two washes with 100 μl of experimental medium, 50 μl of each dye was applied on the cells in distinct wells for 15 min at 37°C. After two washouts of the dyes with 100 μl experimental medium, recordings were carried out with the high-throughput semiautomated plate reader FDSS 7000 EX (Hamamatsu Photonics K.K., Hamamatsu, Japan) equipped with the HighSpeed package software.

Fluorescence signal was recorded through the Hamamatsu EM-CCD ImagEM camera at a sampling interval of 16 ms with the Hamamatsu fluo-3 filter and dichroic mirror kit setting (excitation: 480 nm; emission: 540 nm). The sampling interval can be set from 16 ms to 100 ms. To acquire the signals with a maximal time resolution, the minimal sampling interval of 16 ms was chosen for this study. The entire plate was illuminated at once, and all 96 wells were read at the same time. The average fluorescence levels of the wells were measured and stored simultaneously. Each defined zone of interest (ZOI) corresponded to a well and contained 14×14 pixels encoded in 16 bits with a binning of 2×2. The fluorescence values, referenced here as fluorescence units (FU), were defined on a scale from 0 (no signal) to 65,000 (maximal signal intensity recordable). Drugs were automatically pipetted from a 96-well source plate, and 33 μl was loaded in the wells already containing the cardiomyocytes with 67 μl of media; thus the drug dilution factor was one-third, which was taken into account for the final drug concentration. All experiments were performed at the controlled temperature of 37°C.

Protocol and data analysis. Typically, signal recordings were made at three time points, with the first one for 40 s before drug injection (control condition), the second one for 3 min right after injection of the compounds (acute effects), and the third one at 25 min after injection for 40 s (late effects), leading to a total of 30 min of experiment time. Recorded signals were semiautomatically analyzed with the WaveChecker software (Hamamatsu Photonics K.K.) included in the HighSpeed package. After a manual adjustment of the analysis parameters (e.g., duration of the sample and wells to be analyzed, threshold and duration limit of the peak detection), the software performed an automatic peak detection, counting, averaging of the waveform parameters, and analysis of all 96 wells simultaneously. Typically, data values for a well were averaged from waveforms that arose during 10–20 s of recording and among the different analyzed parameters available. This study mainly focused on the basal fluorescence (BF), beating rate (beats per minute), and waveform amplitude (AMP) and duration at 20%, 50%, and 80% of decay

(WD20, WD50, and WD80, respectively). Wells showing an irregular beating rate (i.e., sudden and limited frequency increases or pauses) before drug application were systematically discarded. The peak duration was defined as the time between the maximal peak value of the fluorescence signal and the return to the resting level so that AMP and duration of eventual drug-induced, arrhythmic, early after-depolarization-like peaks were not included in the results. Every acquisition point and automatically calculated waveform parameter value could be visualized for each well, directly or as a heat map representation of the plate for rapid and intuitive reading.

All data were stored internally and exported as text files. Values, expressed as means or as values relative to basal condition, were calculated with Excel 2010 (Microsoft, Redmond, WA). Graphing, superimposed waveform traces, diastolic slope measurements, and statistical analyses were performed with OriginPro9.1 (OriginLab, Northampton, MA). Diastolic slope measurement for *phase 4* effect detection was done by isolating three consecutive diastolic recording samples for each well in their linear part (after the end of *phase 3* of the preceding waveform and before *phase 0* starting the next one). The samples were fitted individually with a linear function, and the three slope values were averaged for each well. Data are expressed as means $\pm$ SD and were considered statistically different at $P < 0.05$ with a one-way ANOVA test followed by a Bonferroni post hoc test.

RESULTS

Waveform recording: Microscope vs. plate reader signals. Using a standard microscope, we first evaluated the signal generated by a confluent iCell cardiomyocyte monolayer loaded with FV. This initial observation revealed primarily medium-intensity fluorescent signal with spots of brighter or darker cells or small regions (Fig. 1A, *left*). Analysis of single cell-sized ZOIs revealed rhythmic action potential-like waveform activities with varying BF levels and AMPs. Darker spots apparently were associated with a different quality or physiological status of cells with a much larger membrane surface (Fig. 1A, *left*, ZOI 3) that could explain the spatial dilution of their fluorescence. The brighter areas may have contained very compact cells and also fragments of dead cells or depolarized nearly dead cells with little or no rhythmic activity. However, all of the waveforms recorded from any zone of the illuminated area were synchronized and showed the same time course and duration (Fig. 1A, *right*). Consequently, analysis of the signal obtained from the illuminated area revealed waveforms with an average BF and AMP between low- and high-fluorescent intensity areas exactly superimposed on each other. Thus
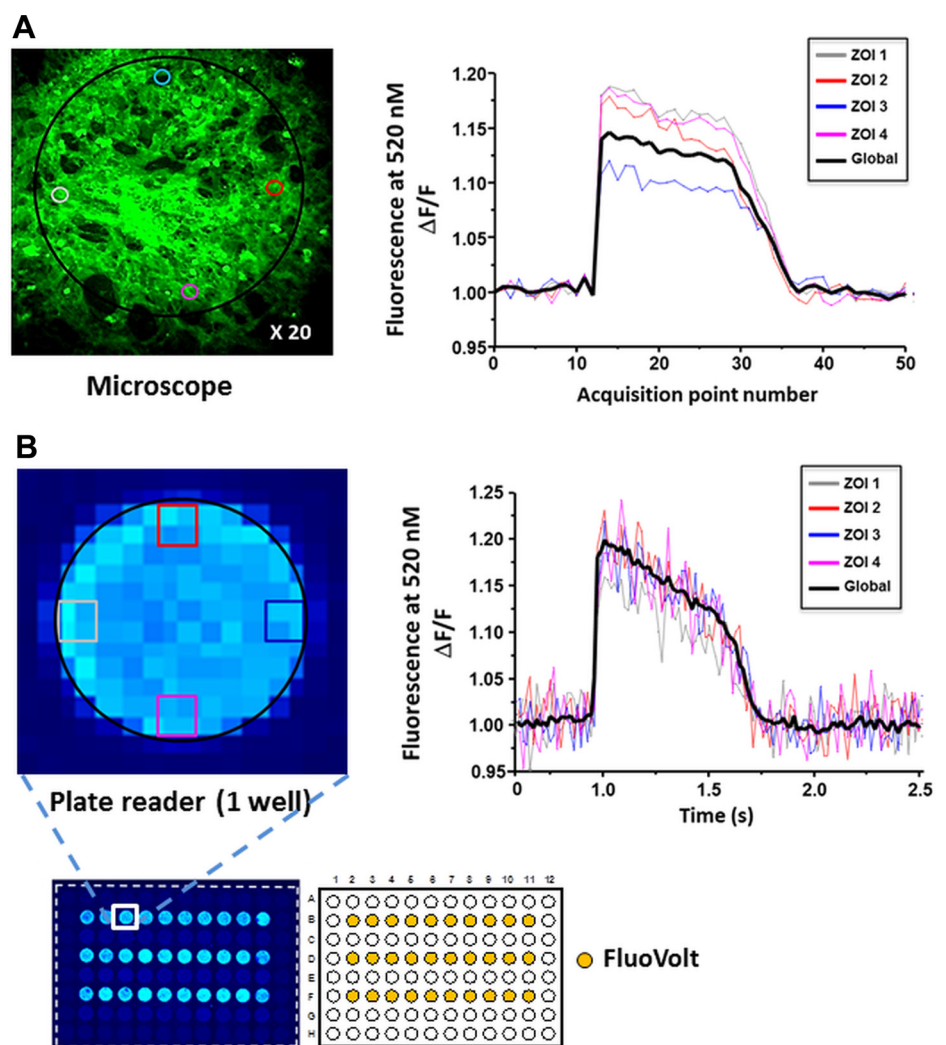

Fig. 1. Microscope and plate reader-based FluoVolt signal recording. *A*: confluent human induced pluripotent stem cells (hiPSC)-derived cardiomyocyte (iCell) monolayer loaded with the FluoVolt (FV) dye and observed with a fluorescence microscope at 520 nm (*left*). Four zones of interest (ZOIs) were defined (colored circles on *left*). The relative fluorescent light value was calculated over time for each zone and compared with the global fluorescence in the well (*right*). *B*: confluent iCell monolayer in a 96-well plate loaded with the FV dye and observed with the FDSS 7000 EX plate reader at 520 nm (*left*). Four ZOIs were defined (colored squares on *left*). The relative fluorescent light value was calculated over time for each zone and compared with the global fluorescence in the well (*right*).

electrical signals reported by FV from a large area of a confluent cardiomyocyte monolayer seemed to closely reflect the signal from individual cells within the monolayer. Of note, except for the AMP and BF discrepancies mostly from heterogeneous dye loading or cell physiological status, the individual electrical waveforms showed an apparent homogeneous electrical activity phenotype that likely resulted from a tight coupling of the cells synchronizing and averaging their membrane potential.

Second, with the same approach, we analyzed the FV signal recorded in a 96-single-well format using the FDSS 7000 EX plate reader. As anticipated, four pixel-sized ZOIs within the same well (Fig. 1B, left) also showed superimposed and synchronized waveforms with the total well signal suggesting that the waveform recorded from a whole well closely reflected the local signal in the cardiomyocyte monolayer (Fig. 1B, right).

Both recording techniques highlighted a high FV BF. Because the AMP of a waveform in relative fluorescence value (ΔF/F) during a beat is about 0.15 to 0.20, BF represented about 80% of the total signal.

Effect of cell density, dye concentration, and DMSO. The impact of cell seeding density and dye concentration on FV signal was investigated in 96-well plate format. Five seeding densities of iCells ranging from 2,500 to 60,000 cells per well were tested. The FV signal was readable at 20,000 cells per well (Fig. 2A), which interestingly corresponds to the lowest number of cells resulting in a fully confluent cell monolayer. At 10,000 cells per well, a weaker and irregular signal was observed, probably originating from large heterogeneous cell clusters. Higher densities did not influence the duration and the beating rate observed (data not shown), but the ratio between the BF and the AMP of the waveform tended to improve slightly, whereas both AMP and resting fluorescence increased significantly with cell density. This effect could be related to the increase in the cell density associated with an increase in total cell membrane surface area where FV localizes.

The highest concentration of the dye (see MATERIALS AND METHODS), d1, led to sudden beating frequency increases or pauses in two of three wells during the first recording and was then discarded. The BF slightly increased during the first 30
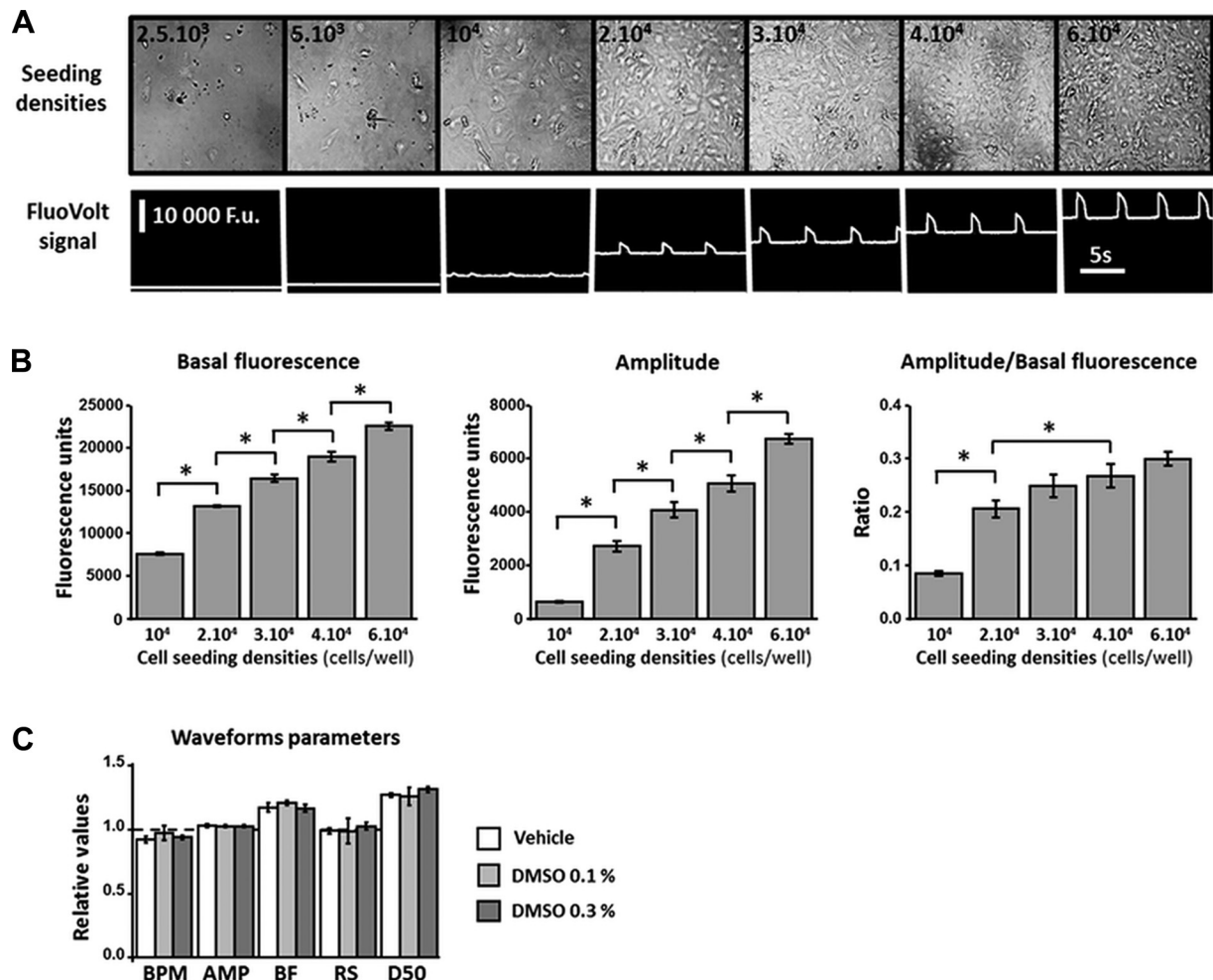

Fig. 2. Effect of the hiPSC-derived cardiomyocyte cell density and the DMSO concentration on FV signal recording in a 96-well plate. *A*: representative images (×20 objective) of wells seeded with iCell cardiomyocytes from 2.5×10^3 to 6×10^4 cells/well (*top*) associated with their corresponding single-well FV fluorescence signal acquired using the plate reader (*bottom*). *B*: values of basal fluorescence (BF), amplitude (AMP), and ratio of AMP over BF of FV waveforms acquired in triplicate for each seeding density. *Significant differences between mean values ($P < 0.05$). *C*: values of various waveform parameters including beats/min (BPM), AMP, BF, rising slope (RS), and waveform duration at 50% of decay (D50) obtained from a 30-min experiment and expressed as relative data compared with the values at the beginning of the experiment in vehicle (open bars), 0.1% DMSO (light shaded bars), and 0.3% DMSO (dark shaded bars) in triplicate for each condition.

min at all concentrations, whereas the AMP tended to decrease over time (Fig. 3A). The ratio of AMP vs. BF level remained close to 0.2 for all concentrations with a slight tendency to decrease over time; however, the BF level remained high for all dye concentrations tested. Beating rate decreased during the first 90 min, and a parallel increase of WD80 simultaneously developed (Fig. 3B). This effect was not observed with the calcium-sensitive dyes in the same experimental conditions (data not shown), suggesting that it might be related to FV itself. However, decreasing the concentration of the dye did not diminish this phenomenon for dilutions higher than d2, suggesting that other parameters of the experimental condition may also have been involved, such as removal of the cell culture media, for example. Forty-second or even 3-min recordings did not led to particular rhythm disturbances or waveform duration modification in our experimental condition; we therefore concluded that a putative phototoxic effect was low and not involved in our results.

DMSO was tested at 0.1% and 0.3% in triplicate in a typical 30-min experiment and had no effect in our experimental conditions on the different parameters calculated from the waveforms (Fig. 2C). BF level, AMP, and their ratio, as well as the rising slope (which is indirectly related to AMP), are susceptible to variation among wells with cell density and morphology, dye loading, and time. Comparisons to the time-equivalent vehicle application in a plate therefore are not recommended, and these waveform parameters are better expressed as values relative to the basal condition for each well.

Accuracy and sensibility of FV electrophysiological signal recording. The prototypical cardiac action potential can be temporally decomposed in five successive phases that correspond to the sequential activities of the main cardiac ion channels [for review see Grant et al. (4)]. To challenge the pharmacological relevance of the assay, we studied the effect of well-characterized cardiotropic drugs that modulate the ventricular cardiac action potential phases through distinct electrophysiological mechanisms.

The effect of lidocaine, a local anesthetic that blocks the fast sodium current involved in the fast-depolarization phase or *phase 0* of the cardiac action potential, was investigated using six concentrations from 1.5 to 50.0 µM in duplicate. Although spontaneous beating rhythm decreased and became irregular (pauses or sudden beating frequency changes) with increasing doses of the drug, because of the altered excitability and conductivity in the cardiomyocyte monolayer, a decrease in the waveform rising slope was observed at 25 and 50 µM, which was significant at 50 µM (Fig. 4A and C). With consideration of the imaging-acquisition and the data-processing time (16 ms), only two to three data points could be acquired during the fast rising slope of the waveforms (Fig. 4A in the magnified trace). Although this low number could be limiting for detecting small effects, it appeared sufficient to characterize moderate to high sodium current-blocking activities.

A set of four drugs that increase or decrease the duration of the plateau *phase 2* or repolarization *phase 3* of the action potential was tested in a single dose in triplicate (Table 1) in three different plates. The human ether-a-go-go-related gene (hERG) potassium channel blocker dofetilide, which epitomizes the most commonly studied drug-induced proarrhythmic effect, significantly increased WD50 and WD80 at 5 nM compared with vehicle, as classically reported (Table 1, Fig. 4B). Some early after-depolarization-like activities could also
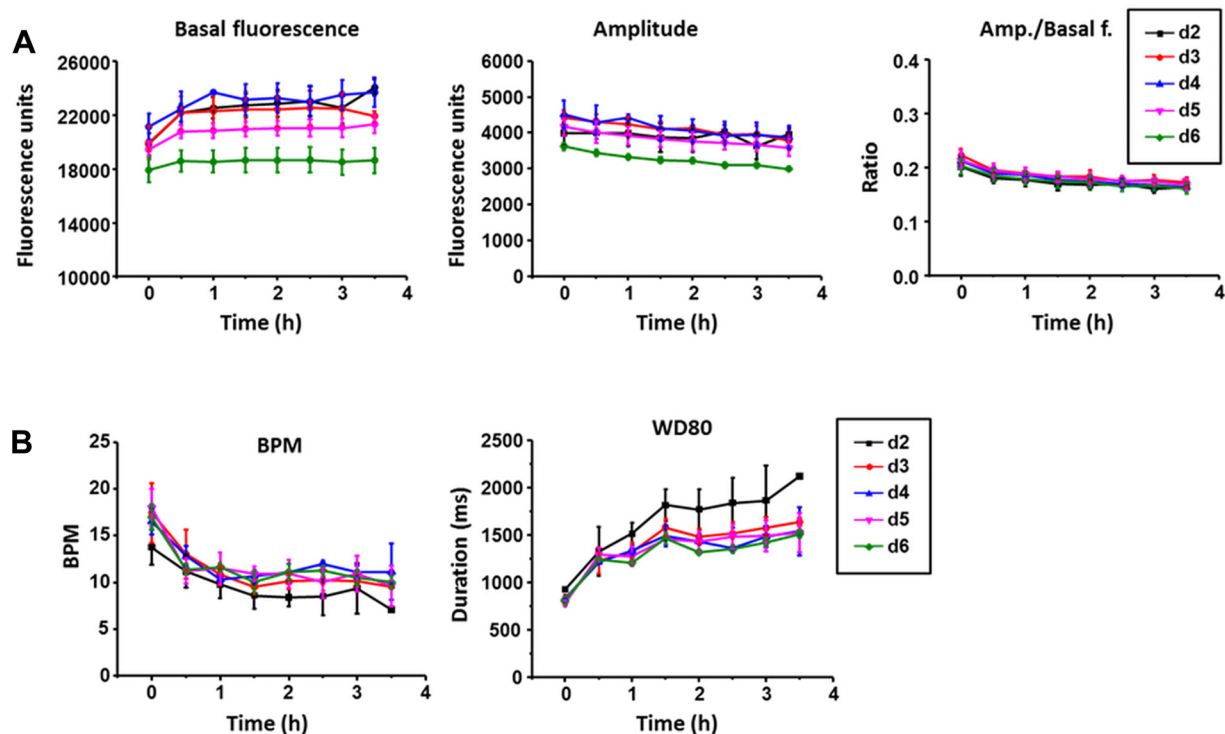

Fig. 3. Effects of the FV concentration on various iPSC-derived cardiomyocyte cellular parameters over time. *A*: effect of 5 dilutions of the FV dye (d2 to d6) on basal fluorescence level (*left*), amplitude (*middle*), and ratio of amplitude vs. basal fluorescence (*right*) recorded every 30 min for 40 s for 3.5 h on iPSC-derived cardiomyocytes (triplicate well). *B*: effect of 5 dilutions of the FV dye (d2 to d6) on BPM (*left*) and duration of the waveforms at 80% of decay (WD80) (*right*) recorded every 30 min for 40 s for 3.5 h on hiPSC-derived cardiomyocytes (triplicate well).
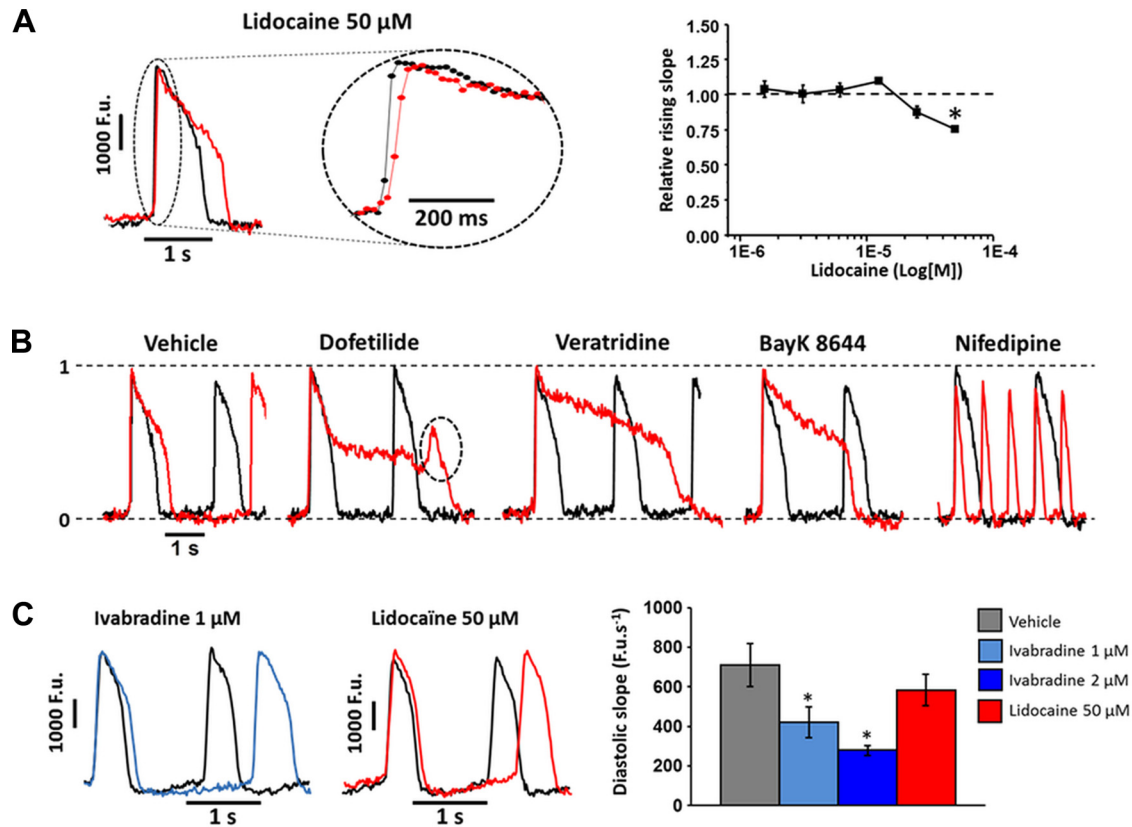
Fig. 4. Drug effects on the different phases of the cardiac action potential in hiPSC-derived cardiomyocytes. *A*: representative FV waveform trace recorded from hiPSC-derived cardiomyocytes (iCell) before (black) and 30 min after (red) treatment with 50 μM lidocaine (*left*), including an enlarged view of the fast-depolarization phase (*middle*). Dose-dependent effect of lidocaine at 1.50, 3.12, 6.25, 12.50, 25.00, and 50.00 μM on the RS expressed in relative value to basal condition (*right*). *Significantly different from value at 1.5 μM ($P < 0.05$). *B*: representative traces of Fv waveform recorded before (black) and 30 min after (red) treatment of iCell with vehicle, dofetilide (20 nM), veratridine (1 μM), Bay K8644 (1 μM), and nifedipine (1 μM). The dashed line circle on the dofetilide-treated signal shows an early after-depolarization-like activity. *C*: representative traces of FV waveform recorded before (black) and 30 min after (red) treatment of hiPSC-derived cardiomyocytes (Cor.4U) with ivabradine (1 μM) (light blue) and lidocaine (50 μM) (red) (*left*). Values of depolarization slope expressed in fluorescence units per s (FU/s) 30 min after application of vehicle (gray), ivabradine (1 μM) (light blue), ivabradine (2 μM) (blue), and lidocaine (50 μM) (red). *Significantly different from vehicle ($P < 0.05$).

be seen (Fig. 4*B*, dashed circle). Interestingly, WD20 was unaffected because hERG is involved only at the end of the plateau phase and does not contribute to the early part of the repolarization process in the heart [for review see Vandenberg et al. (23)]. Dofetilide was also tested from 1.5 to 50.0 nM (6 concentrations in duplicate) and showed a dose-dependent

increase at WD80 from 1.0 to 12.5 nM, whereas, for WD20, AMP and rising slope were not or were weakly affected. A decrease in beating frequency was also observed (Fig. 5*A*). Inversely, veratridine, which prolongs the ventricular action potential by enhancing the late component of the sodium current, triggering *phase 0* of the action potential [see for

Table 1. *FluoVolt waveform parameter values for a selection of reference compounds*

Drug	n	BPM	AMP	R Slope	RF	WD20, ms	WD80, ms	Values
Control	9	0.3 ± 0.89	—	—	—	328.91 ± 39.74	894.88 ± 116.08	Absolute
		0.88 ± 0.12	0.97 ± 0.06	0.94 ± 0.09	1.06 ± 0.02	1.01 ± 0.1	1.18 ± 0.25	Relative
Dofetilide (5 nM)	9	14.98 ± 1.88	—	—	—	301.66 ± 57.87	2455.48 ± 417.46*	Absolute
		0.62 ± 0.09	0.92 ± 0.05	0.85 ± 0.13	1.07 ± 0.04	0.97 ± 0.07	3.41 ± 0.78*	Relative
Veratridine (1 μM)	9	11.91 ± 2.55	—	—	—	500.98 ± 125.13*	2577.76 ± 1001.91*	Absolute
		0.51 ± 0.14	1.00 ± 0.08	0.98 ± 0.08	1.04 ± 0.04	1.63 ± 0.65*	3.53 ± 1.62*	Relative
Bay K8644 (1 μM)	7	13.79 ± 1.13	—	—	—	584.19 ± 90.06*	2058.26 ± 301.37*	Absolute
		0.56 ± 0.09	1.03 ± 0.08	0.99 ± 0.1	1.04 ± 0.04	1.87 ± 0.18*	2.85 ± 0.57*	Relative
Nifedipine (1 μM)	9	70.52 ± 11.85*	—	—	—	72.98 ± 4.65*	251.37 ± 20.15	Absolute
		2.85 ± 0.31*	0.86 ± 0.04*	0.97 ± 0.05	1.04 ± 0.03	0.23 ± 0.04*	0.34 ± 0.06	Relative

Values are expressed as means ± SD. Mean FluoVolt parameter values were obtained in triplicate of each condition from 3 independent plates and expressed as absolute values or as values relative to basal condition. Two wells treated with Bay K8644 were discarded due to irregular beating rate. BPM, beats/min; AMP, amplitude; R Slope, rising slope; RF, resting fluorescence; WD20 and WD80, waveform duration at 20 and 80% of decay, respectively. *Significantly different from control condition ($P < 0.05$).
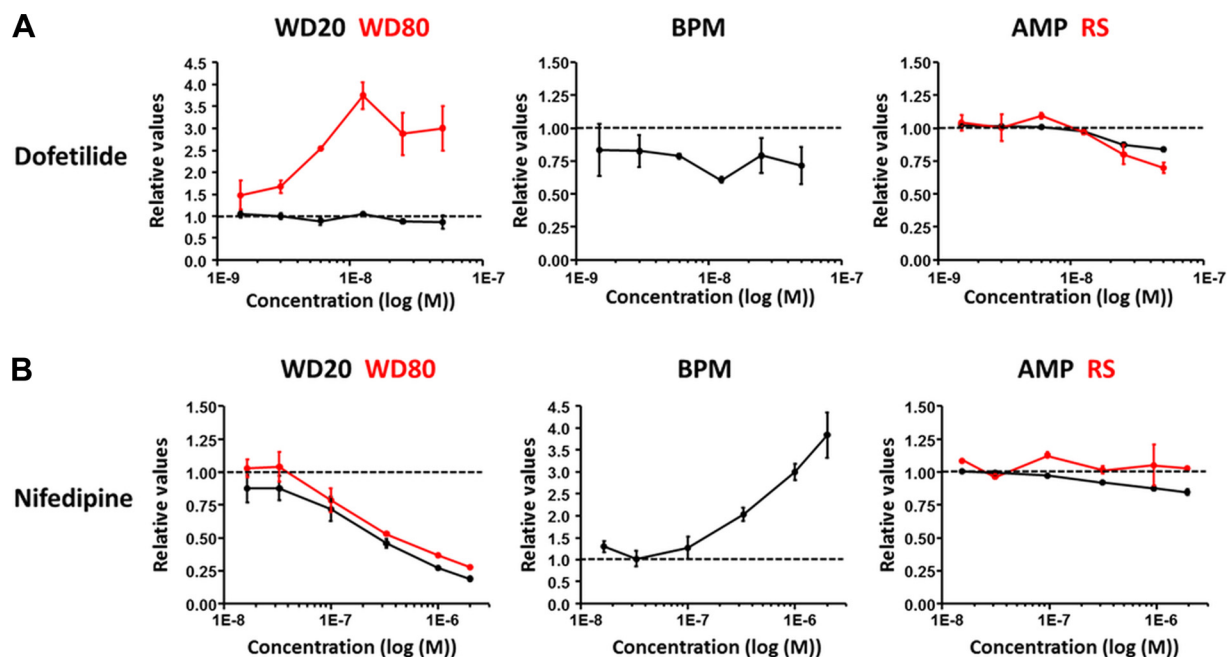
Fig. 5. Dose effects of dofetilide and nifedipine on hiPSC-derived cardiomyocytes. *A*: WD20, WD80, BPM, AMP, and RS parameters (relative to basal) calculated from FV waveforms record 30 min after treatment of hiPSC-derived cardiomyocytes with increasing doses of dofetilide (1.5, 3.1, 6.2, 12.5, 25.0, and 50.0 nM). *B*: WD20, WD80, BPM, AMP, and RS parameters (relative to basal) calculated from FV waveforms recorded 30 min after treatment of hiPSC-derived cardiomyocytes with increasing doses of nifedipine (0.016, 0.033, 0.100, 0.330, 1.000, and 2.000 μM).

review Shryock et al. (17)], significantly increased both early and late phases of the repolarization process (Table 1, Fig. 4*B*). This was also the case for the calcium channel agonist Bay K8644, as reported in ventricular preparations (16). Overall, these results demonstrated that the recording of the electrical activity from a whole well with FV enables discriminating pure *phase 3*-prolonging drugs (dofetilide) from *phase 0*- or *phase 2*-prolonging drugs (veratridine or Bay K8644).

Finally, the calcium channel blocker nifedipine (1 μM) induced a significant beating frequency increase, a significant shortening of the early phase of the waveform, and a slight reduction in the waveform AMP (Table 1). In the six-concentration dose-effect study done in duplicate, there was a pronounced dose-dependent decrease in WD20 and WD80 and a marked beating rate increase, accompanied by a modest AMP decrease (Fig. 5*B*). These results are in agreement with previous data generated with calcium channel blockers on the same cell line using microelectrode array and/or impedance measurement (5, 10). Ultimately, the data in Table 1 clearly demonstrate that parameters significantly differing from those of the vehicle condition do so regardless of their expression as either absolute values (except for AMP, rising slope, or BF, as noted) or relative to basal values, showing that the interplate data variation is very limited. Moreover, drug dose-dependent-induced effects are clearly seen in duplicate with small standard deviations, demonstrating that intraplate data variation is also very low.

This new approach in a 96-well plate format provides access to an action potential-related waveform in real time and enables precise electrophysiological mechanism characterization. This type of investigation, notably on early and late repolarization effects, could be more difficult to perform, however, with an indirect signal derived with methods such as micro-

electrode arrays. To further illustrate this point, we recorded FV waveforms from Axiogenesis Cor.4U hiPSC-derived cardiomyocytes, which show a higher beating rate and a more prominent *phase 4* (diastolic depolarization slope of the cardiac action potential) than iCell cardiomyocytes, suggesting a higher pacemaker current activity (22). Ivabradine, a specific blocker of the pacemaker current generated by the hyperpolarization-activated cyclic nucleotide-gated channel (HCN) ion channel family, was tested at 1 and 2 μM in quadruplicate. After 30 min, this drug significantly slowed the spontaneous Cor.4U cell beating rhythm (31.19 ± 0.94 beats/min for 1 μM ivabradine, 23.19 ± 0.74 for 2 μM ivabradine compared with 42.46 ± 2.07 for vehicle control, respectively). In the same conditions, 50 μM lidocaine, a blocker of the fast sodium current contributing to the depolarization phase of the cardiac action potential, also significantly reduced the Cor.4U cell spontaneous beating rate (down to 36.12 ± 1.02 beats/min compared with 42.46 ± 2.07 for vehicle control). A manual analysis revealed that the slowing effect of ivabradine, as reported on sinus node multicellular preparations with the microelectrode technique (21), was accompanied by a significant decrease in the diastolic depolarization slope of the FV waveforms compared with vehicle (values expressed in FU/s, were 420.03 ± 77.05 at 1 μM and 279.16 ± 24.85 at 2 μM for ivabradine vs. 710.30 ± 110.25 for vehicle control; Fig. 4*C*, *right*); this pattern was not the case for lidocaine (Fig. 4*C*). Although a small inhibitory effect on HCN channels explaining the nonsignificant decrease of the *phase 4* slope (to 584.16 ± 79.55 FU/s) could not be ruled out (20), lidocaine rather prolonged *phase 4* of the cardiomyocyte electrical activity, whereas ivabradine slowed it down dose dependently. Additionally, these results strongly suggest that HCN channels are functionally involved in the generation of *phase 4* of the action

potential of the Cor.4U cells and participate in the regulation of their spontaneous beating rate.

Implementation of the calcium signaling recording. As a consequence of drug cardiotropic effect or pathological issues, altered ion channel activity can lead to changes in calcium homeostasis, and, inversely, arrhythmias can occur from perturbations of the calcium cycling within the cardiomyocyte (24). Electrical signal recording could therefore be effectively complemented by calcium transient activity recording to better characterize pharmacological responses of hiPSC-derived cardiomyocytes. Calcium transient activity signal could be captured along with FV in separate wells but in the same plate using calcium-sensitive dyes such as fluo-4 or Cal520, which have overlapping excitation and emission wavelengths, and then recording them in a concomitant manner. The calcium signal acquisition in a whole well benefited from the same spatial homogeneity as the electrical signal. Although the two fluorescent signals did not come from the same wells, there was a nice temporal correlation of the drug-induced events that enabled parallel tracking of the pharmacological effects. Figure 6 shows an example of acute dofetilide-induced arrhythmia activity with early after-depolarization-like activities arising simultaneously from an FV and a calcium-sensitive dye-loaded well. This example also shows that arrhythmic behavior is achievable in whole-well waveform recording. Some discrepancies in drug-induced waveform alteration proportion or arrhythmic event number between the electrical and calcium signals were occasionally observed. They were related to variability or to signal-specific or dye-specific singularities.

Although global waveform duration of both signals varies similarly in response to drugs (19), a similar electrophysiological profile can correspond to opposite calcium waveform alteration depending on their pharmacological mechanism. For example, nifedipine (1 μM) and ouabain (5 μM), a cardiac glycoside that blocks the Na^+/K^+ ATPase pump, both increased beats/min and decreased FV waveform WD20, WD80, and AMP similarly, making them undistinguishable (Fig. 7*B*). However, the recording of the calcium signal with the Cal520 dye showed a decrease of AMP, WD20, and rising slope in response to nifedipine, whereas these parameters were increased in response to ouabain (Fig. 7, *A--C*), in agreement with a study on the same cell line using microelectrode array field potential recording (5). Moreover, resting fluorescence level tended to increase during ouabain treatment, as a consequence of calcium overload (Fig. 7, *B* and *C*). This result clearly exemplified the relevance of using a calcium-sensitive dye concomitantly with a voltage-sensitive dye on the same plate to differentiate the pharmacological profiles of compounds.

DISCUSSION

In this study, we demonstrate that the FV dye is a very attractive and well-adapted tool to record electrophysiological events in a spontaneously beating monolayer of hiPSC-derived cardiomyocytes seeded in 96-well plate format. According to our microscope-based investigations, the overall FV signal from an entire well remains qualitatively close to that recorded from a single cell-sized or very small-sized ZOIs. The drawbacks of the probe were a high BF level, an immediate cellular toxicity at the highest concentration, a slowly developing waveform duration lengthening, and a decrease in beats/min that tended to stabilize after 2 h. The low waveform AMP:BF ratio is an intrinsic property of the dye that is close to the reported increase of fluorescence per 100 mV described in the FV kit (20–25%) and for the VoltageFluor sensor family (15). This ratio could be improved by increasing the cellular seeding density. Except for the irregular beating triggered by the highest FV concentration tested, the lower concentration had only a moderate cellular toxicity totally compatible with episodic recordings during >3 h. This effect did not interfere with drug responses and was further mitigated by a three- to fivefold dilution of the dye without compromising the FV signal. A sixfold dilution led to a decrease in the signal AMP.

We were able to record significant drug responses that were in complete agreement with the observations made using other techniques like microelectrode array and/or impedance measurement. Moreover, the level of information extracted from the FV signal in a whole well was sufficiently close to that generated by gold standard genuine action potential recording techniques, such as patch-clamp or intracellular microelectrode techniques, to enable distinction of drugs acting through different electrophysiological mechanisms. Fast-depolarization phase slowing in response to a sodium channel blocker and early- or late-repolarization alteration by different action potential-prolonging drugs were detected with this technique. It was also possible, through a manual data analysis, to characterize and measure the *phase 4* slowing effect of the HCN blocker ivabradine on the pacemaker activity of the Cor.4U cell line. Ultimately, the implementation of the calcium-sensitive dye along with FV proved to be a very effective approach for thoroughly investigating complex pharmacological responses and further helped to mechanically discriminate between compounds.
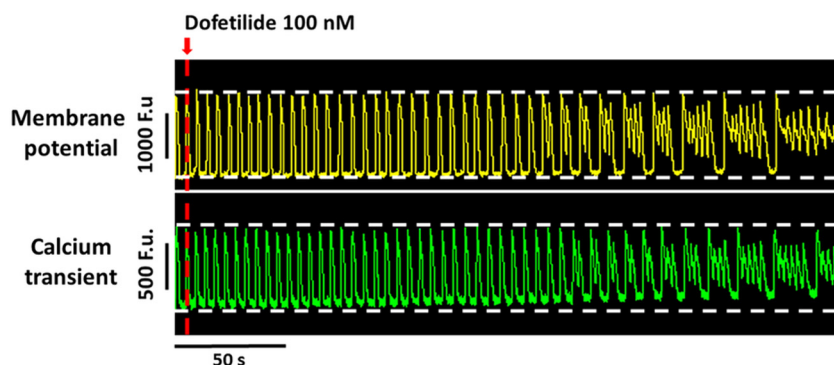

Fig. 6. Simultaneous electrical and calcium transient signal acquisition on dofetilide-treated iPSC-derived cardiomyocytes. Printscreens of FV signal (*top* in yellow) and fluo-4 signal (*bottom* in green) recorded from 2 different wells of the same 96-well plate during injection of dofetilide (100 nM), showing the temporal coincidence of early after-depolarization-like activity arising. The red arrow indicates the moment of the injection of the drug.
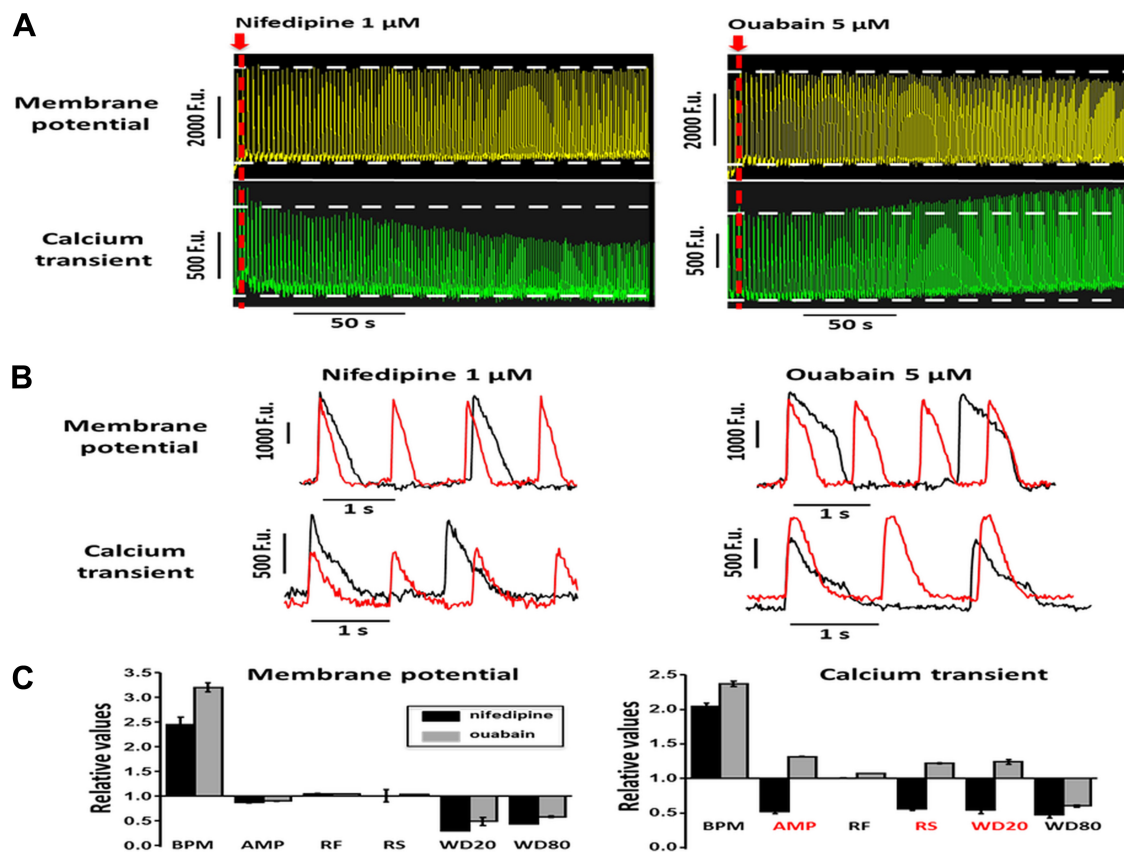
Fig. 7. Effect of nifedipine and ouabain treatment on electrophysiological and calcium signal from hiPSC-derived cardiomyocytes. *A*: printscreens of FluoVolt (*top* yellow traces) and Cal520 (*bottom* green traces) signal recordings in different wells during injection of nifedipine (1 μM) (*left*) and ouabain (5 μM) (*right*). *B*: representative FV (*top*) and Cal520 (*bottom*) waveforms (extracted from wells presented in *A*) acquired 10 s (black) and 3 min (red) after nifedipine (*left*) and ouabain (*right*) treatment. *C*: BPM, AMP, basal fluorescence level (BF), RS, WD20, and WD80 calculated (relative to basal) from the FV (*left*) and Cal520 (*right*) waveforms acquired 3 min after injection of nifedipine (black) and ouabain (gray). The 2 drugs tested differed only in their effect on the Cal520 AMP, BF, and WD20 parameters (in red) that vary in opposite ways. For both graphs, the *y*-axis is centered on the value of 1, which corresponds to no change relative to the basal value.

Although the phenotypic properties of the different sources of hiPSC-derived cardiomyocytes are not in the scope of this study, it is critical to mention that these must be carefully considered for drug profiling. For example, *phase 4* effects would be harder to characterize in a cell line with a poorly defined spontaneous waveform diastolic depolarization slope. Moreover, we characterized the other drug responses based on their qualitative effects on the isolated parameters on the waveforms, but they are susceptible to variation among cell lines and also within a population of hiPSC-derived cardiomyocytes of the same origin. A recent study also using a fluorescent voltage-sensitive dye showed that action potential morphology variability can be somewhat present in fully confluent hiPSC-derived cardiomyocytes but to a lesser extent than when sparsely seeded (2). However, in our experimental conditions and within the limits of our recording time and spatial resolutions, monolayers of beating cardiomyocytes generate homogeneous local and global electrical signals. This strongly suggests that the possible phenotypic heterogeneity among cells is averaged by their tight functional coupling. This finding represents a clear advantage of whole well fluorescence recording because the global electrical and calcium activity leads to reproducible signals and pharmacological responses potentially devoid of the variability that can occur in individual cell-based recordings.

On the basis of a fast imaging process, the frame recording interval of 16 ms is sufficient to record the waveforms with a satisfying time resolution, but the detection of the rapid *phase 0* alterations may lack sensitivity and only detect moderate to high slowing effects. A theoretical doubling of the time resolution might be achievable by a twofold increase in the camera-binning process, but this possibility, which also decreases the spatial resolution, remains to be tested. Another limitation of our approach originates from the high BF level of FV that reduces our ability to detect small global depolarization in response to drugs like ouabain, for example, although it decreases the AMP of the FV waveforms in our conditions. Therefore, the capacity of our assay to detect depolarizing effects needs further investigation. In addition, although some early after-depolarization-like waveforms are observable after proarrhythmic drug injection, the whole-well recording approach theoretically limits our ability to detect local sporadic nonpropagated events like underthreshold delay after depolarizations.

Finally, we conclude that the concomitant implementation of a fast-responding voltage-sensitive dye like FV and a calcium-sensitive dye in the same 96-well plate represents a simple and reliable multiparametric method to investigate both electrophysiological and calcium activity-related effects of candidate drugs. With an automated plate reader that includes semiauto-

mated analysis software, this technique allows high-throughput drug characterization on classic waveform parameters. The quality of the recordings also permits in-depth electrophysiological mechanistic investigations that could be further interpreted through manual analysis. Combined with the use of hiPSC-derived cardiomyocyte cell lines, this approach represents a very attractive alternative to other high-throughput methods for cardiac safety and/or newly discovered drug candidate profiling.

DISCLOSURES

No conflicts of interest, financial or otherwise, are declared by the authors.

AUTHOR CONTRIBUTIONS

S.B., C.S.N., J.-P.S., and F.C. conception and design of research; S.B., C.S.N., V.L., S.C., and F.C. performed experiments; S.B., C.S.N., V.L., and S.C. analyzed data; S.B. and C.S.N. interpreted results of experiments; S.B., C.S.N., V.L., and S.C. prepared figures; S.B., C.S.N., V.L., S.C., J.A.B., O.N., J.-P.S., and F.C. drafted manuscript; S.B., C.S.N., J.A.B., O.N., J.-P.S., and F.C. edited and revised manuscript; S.B., C.S.N., V.L., S.C., J.A.B., O.N., J.-P.S., and F.C. approved final version of manuscript.

REFERENCES

1. **Braam SR, Tertoolen L, van de Stolpe A, Meyer T, Passier R, Mummery CL.** Prediction of drug-induced cardiotoxicity using human embryonic stem cell-derived cardiomyocytes. *Stem Cell Res* 4: 107–116, 2010.
2. **Du DT, Hellen N, Kane C, Terracciano CM.** Action potential morphology of human induced pluripotent stem cell-derived cardiomyocytes does not predict cardiac chamber specificity and is dependent on cell density. *Biophys J* 108: 1–4, 2015.
3. **Gibson JK, Yue Y, Bronson J, Palmer C, Numann R.** Human stem cell-derived cardiomyocytes detect drug-mediated changes in action potentials and ion currents. *J Pharmacol Toxicol Methods* 70: 255–267, 2014.
4. **Grant AO.** Cardiac ion channels. *Circ Arrhythm Electrophysiol* 2: 185–194, 2009.
5. **Guo L, Abrams RM, Babiarz JE, Cohen JD, Kameoka S, Sanders MJ, Chiao E, Kolaja KL.** Estimating the risk of drug-induced proarrhythmia using human induced pluripotent stem cell-derived cardiomyocytes. *Toxicol Sci* 123: 281–289, 2011.
6. **He JQ, Ma Y, Lee Y, Thomson JA, Kamp TJ.** Human embryonic stem cells develop into multiple types of cardiac myocytes: action potential characterization. *Circ Res* 93: 32–39, 2003.
7. **Hescheler J, Halbach M, Egert U, Lu ZJ, Bohlen H, Fleischmann BK, Reppel M.** Determination of electrical properties of ES cell-derived cardiomyocytes using MEAs. *J Electrocardiol* 37, *Suppl*: 110–116, 2004.
8. **Himmel HM.** Drug-induced functional cardiotoxicity screening in stem cell-derived human and mouse cardiomyocytes: effects of reference compounds. *J Pharmacol Toxicol Methods* 68: 97–111, 2013.
9. **Hu N, Wang T, Wang Q, Zhou J, Zou L, Su K, Wu J, Wang P.** High-performance beating pattern function of human induced pluripotent stem cell-derived cardiomyocyte-based biosensors for hERG inhibition recognition. *Biosens Bioelectron* 67: 146–153, 2015.
10. **Jonsson M, Wang Q, Becker B.** Impedance-based detection of beating rhythm and proarrhythmic effects of compounds on stem cell-derived cardiomyocytes. *Assay Drug Dev* 9: 590–599, 2016.
11. **Lee P, Klos M, Bollensdorff C, Hou L, Ewart P, Kamp TJ, Zhang J, Bizy A, Guerrero-Serna G, Kohl P, Jalife J, Herron TJ.** Simultaneous voltage and calcium mapping of genetically purified human induced pluripotent stem cell-derived cardiac myocyte monolayers. *Circ Res* 110: 1556–1563, 2012.
12. **Leyton-Mange JS, Mills RW, Macri VS, Jang MY, Butte FN, Ellinor PT, Milan DJ.** Rapid cellular phenotyping of human pluripotent stem cell-derived cardiomyocytes using a genetically encoded fluorescent voltage sensor. *Stem Cell Reports* 2: 163–170, 2014.
13. **Lopez-Izquierdo A, Warren M, Riedel M, Cho S, Lai S, Lux RL, Spitzer KW, Benjamin IJ, Tristani-Firouzi M, Jou CJ.** A near-infrared fluorescent voltage-sensitive dye allows for moderate-throughput electrophysiological analyses of human induced pluripotent stem cell-derived cardiomyocytes. *Am J Physiol Heart Circ Physiol* 307: H1370–H1377, 2014.
14. **Ma J, Guo L, Fiene SJ, Anson BD, Thomson JA, Kamp TJ, Kolaja KL, Swanson BJ, January CT.** High purity human-induced pluripotent stem cell-derived cardiomyocytes: electrophysiological properties of action potentials and ionic currents. *Am J Physiol Heart Circ Physiol* 301: H2006–H2017, 2011.
15. **Miller EW, Lin JY, Frady EP, Steinbach PA, Kristan WB Jr, Tsien RY.** Optically monitoring voltage in neurons by photo-induced electron transfer through molecular wires. *Proc Natl Acad Sci USA* 109: 2114–2119, 2012.
16. **Rampe D, Anderson B, Rapien-Pryor V, Li T, Dage RC.** Comparison of the in vitro and in vivo cardiovascular effects of two structurally distinct Ca++ channel activators, BAY K 8644 and FPL 64176. *J Pharmacol Exp Ther* 265: 1125–1130, 1993.
17. **Shryock JC, Song Y, Rajamani S, Antzelevitch C, Belardinelli L.** The arrhythmogenic consequences of increasing late INa in the cardiomyocyte. *Cardiovasc Res* 99: 600–611, 2013.
18. **Sirenko O, Crittenden C, Callamaras N, Hesley J, Chen YW, Funes C, Rusyn I, Anson B, Cromwell EF.** Multiparameter in vitro assessment of compound effects on cardiomyocyte physiology using iPSC cells. *J Biomol Screen* 18: 39–53, 2013.
19. **Spencer CI, Baba S, Nakamura K, Hua EA, Sears MA, Fu CC, Zhang J, Balijepalli S, Tomoda K, Hayashi Y, Lizarraga P, Wojciak J, Scheinman MM, Aalto-Setala K, Makielski JC, January CT, Healy KE, Kamp TJ, Yamanaka S, Conklin BR.** Calcium transients closely reflect prolonged action potentials in iPSC models of inherited cardiac arrhythmia. *Stem Cell Reports* 3: 269–281, 2014.
20. **Tamura A, Ogura T, Uemura H, Reien Y, Kishimoto T, Nagai T, Komuro I, Miyazaki M, Nakaya H.** Effects of antiarrhythmic drugs on the hyperpolarization-activated cyclic nucleotide-gated channel current. *J Pharm Sci* 110: 150–159, 2009.
21. **Thollon C, Bedut S, Villeneuve N, Coge F, Piffard L, Guillaumin JP, Brunel-Jacquemin C, Chomarat P, Boutin JA, Peglion JL, Vilaine JP.** Use-dependent inhibition of hHCN4 by ivabradine and relationship with reduction in pacemaker activity. *Br J Pharmacol* 150: 37–46, 2007.
22. **van den Heuvel NH, van Veen TA, Lim B, Jonsson MK.** Lessons from the heart: mirroring electrophysiological characteristics during cardiac development to in vitro differentiation of stem cell derived cardiomyocytes. *J Mol Cell Cardiol* 67: 12–25, 2014.
23. **Vandenberg JI, Perry MD, Perrin MJ, Mann SA, Ke Y, Hill AP.** hERG K(+) channels: structure, function, and clinical significance. *Physiol Rev* 92: 1393–1478, 2012.
24. **Wagner S, Maier LS, Bers DM.** Role of sodium and calcium dysregulation in tachyarrhythmias in sudden cardiac death. *Circ Res* 116: 1956–1970, 2015.
25. **Warren M, Spitzer KW, Steadman BW, Rees TD, Venable P, Taylor T, Shibayama J, Yan P, Wuskell JP, Loew LM, Zaitsev AV.** High-precision recording of the action potential in isolated cardiomyocytes using the near-infrared fluorescent dye di-4-ANBDQBS. *Am J Physiol Heart Circ Physiol* 299: H1271–H1281, 2010.
26. **Zeevi-Levin N, Itskovitz-Eldor J, Binah O.** Cardiomyocytes derived from human pluripotent stem cells for drug screening. *Pharmacol Ther* 134: 180–188, 2012.
27. **Zhang XH, Haviland S, Wei H, Saric T, Fatima A, Hescheler J, Cleemann L, Morad M.** Ca2+ signaling in human induced pluripotent stem cell-derived cardiomyocytes (iPS-CM) from normal and catecholaminergic polymorphic ventricular tachycardia (CPVT)-afflicted subjects. *Cell Calcium* 54: 57–70, 2013.